Materials Research Proceedings 41 (2024) 2617-2627 https://doi.org/10.21741/9781644903131-287

Characterization of recycled polyethylene terephthalate (rPET) – impact of proportion of virgin and recycled PET on mechanical strength

NGUYEN Thanh-Tung[1,a*], LUO Yun-Mei[1,b] , CHEVALIER Luc[1,c], LESUEUR François[2,d], DERRIEN Mikael[2,e]

[1]Université Gustave Eiffel, Laboratoire Modélisation et Simulation Multi Echelle, MSME UMR 8208 CNRS, 5 bd Descartes, 77545 Marne-la-Vallée, France

[2]SIDEL Blowing & Services, Avenue de la Patrouille de France, C5 60627 Octeville sur mer, France

[a]thanh-tung.nguyen@univ-eiffel.fr, [b]yun-mei.luo@univ-eiffel.fr, [c]luc.chevalier@univ-eiffel.fr, [d]francois.lesueur@sidel.com, [e]mikael.derrien@sidel.com

Keywords: Recycled PET, Characterization, Mechanical Strength, Bi-Axial Test

Abstract. Polyethylene terephthalate (PET) is a standard plastic with the highest consumption in the food packaging industry. The large amount of bottles produced makes imperative the search for the recycled PET (rPET). However, the recycling procedure generates the modifications of the mechanical, thermal and optical properties from virgin PET to recycled one. In this study, Digital Image Correlation method associated to numerical simulation is used to identify the mechanical properties of the bottles. The effects of various recycled PET ratios on the mechanical properties of bottles are discussed.

Introduction

The massive production of PET plastic bottles generates very visible pollution problems around which negative communication endangers the future of the packaging industry. Recycling is certainly a response to this situation in order to improve the image of the polymer industry by working on the sorting and recycling sectors. Producing new bottles from old ones is a simple idea unless the properties of the product are not too degraded compared to a new bottle.

Numerous works have been carried out [1-5] to capture the mechanical and thermal behavior of rPET. In this work we look for the correlation between the rate of recycled and the induced mechanical behavior. It is well known that the blowing process reinforces the mechanical strength and rigidity of the material [6-9] and our purpose is to measure the induced elastic properties in order to answer whether if the recycled PET reduces or not these induced properties.

In the first part, we will present the material, the specimen and the method used to measure the wanted properties. Then, in the second part, we will present and discuss the obtained results.

Material and identification methods

The material used as the virgin PET is RAMAPET N180. Its glass transition temperature is 78+/-2°C and its intrinsic viscosity is 0.80+/-0.02 dl/g. The recycled PET is referenced MOPET and its intrinsic viscosity is 0.85+/-0.02 dl/g. Characteristics are detailed in the Tables of the Appendix.

Four types of bottles were blown by Sidel with different mass fraction of recycled PET (see Table 1). The geometry of the preform is illustrated on Fig.1a. The final diameter of the bottle set on the blowing apparatus shown on Fig.1b is 70mm and the measured thickness in the central region is 0.3mm.

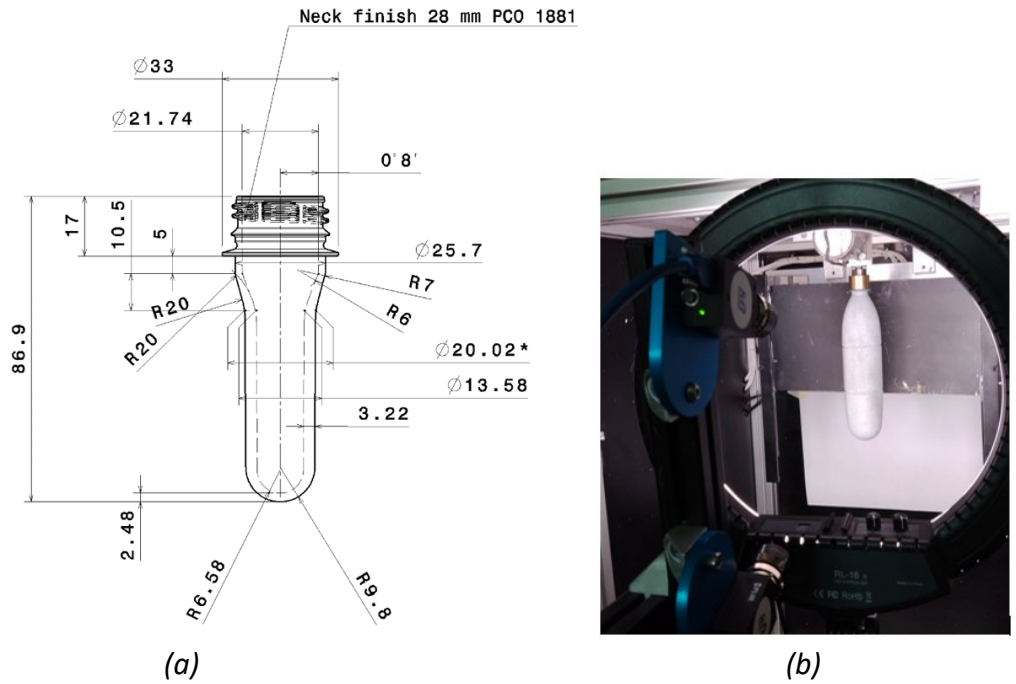

Figure 1. (a) The preform geometry, (b) the final bottle during the internal pressure test

Consequently, one can evaluate the radial elongation λ_r=5.15 and the thickness contraction λ_e=0.093. By assuming the volume conservation, one can estimate the longitudinal elongation in the central region λ_z=2.09.

Table 1: Four different types of bottle

	MOPET (recycled)	**N180 (virgin)**
Bottle 1	0%	100%
Bottle 2	25%	75%
Bottle 3	50%	50%
Bottle 4	100%	0%

Two different methods are used to identify the mechanical properties of the blown bottles. Both are based on measuring strains with a digital image correlation (DIC) technique [10]. For the nondestructive method, a blowing apparatus developed in laboratory MSME is used in order to put the bottle under pressure (Fig.1b). We focus on a region of interest (ROI) where the DIC provides the components of the displacement field as shown on Fig.2.

This method has already been detailed in previous paper of authors [11] for example. To make sure of the linearity, we increase the pressure by step of 0.5 bar from 0 to 5bar and the strains and stresses are obtained at each step. Considering the cylindrical central zone, one can evaluate the stresses σ_r and σ_z from the internal pressure P:

$$\sigma_z = \frac{PR}{2e}, \sigma_\theta = \frac{PR}{e} \quad (1)$$

where R the radius in the cylindrical part of the bottle (35mm) and e the thickness of the same part (0.3mm).

This leads to two relations from where one can evaluate the modulus E_θ and E_z if the Poisson's ratio is known.

$$\varepsilon_z = \frac{PR}{2eE_z}\left(1-2\frac{\upsilon_{\theta z}}{E_\theta}E_z\right), \varepsilon_\theta = \frac{PR}{eE_\theta}\left(1-\frac{\upsilon_{\theta z}}{2}\right) \quad (2)$$

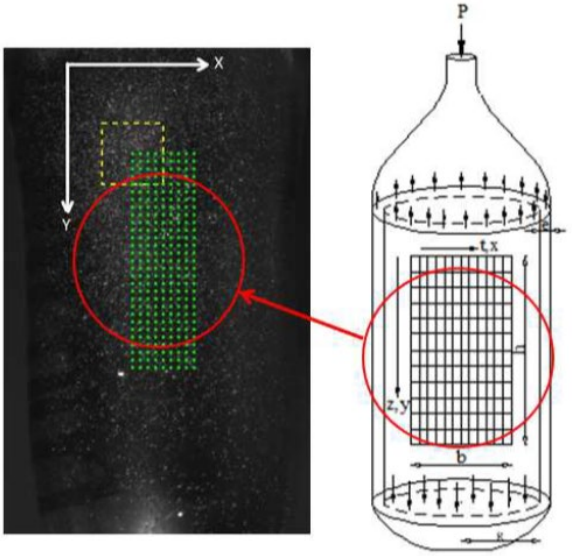

(a)

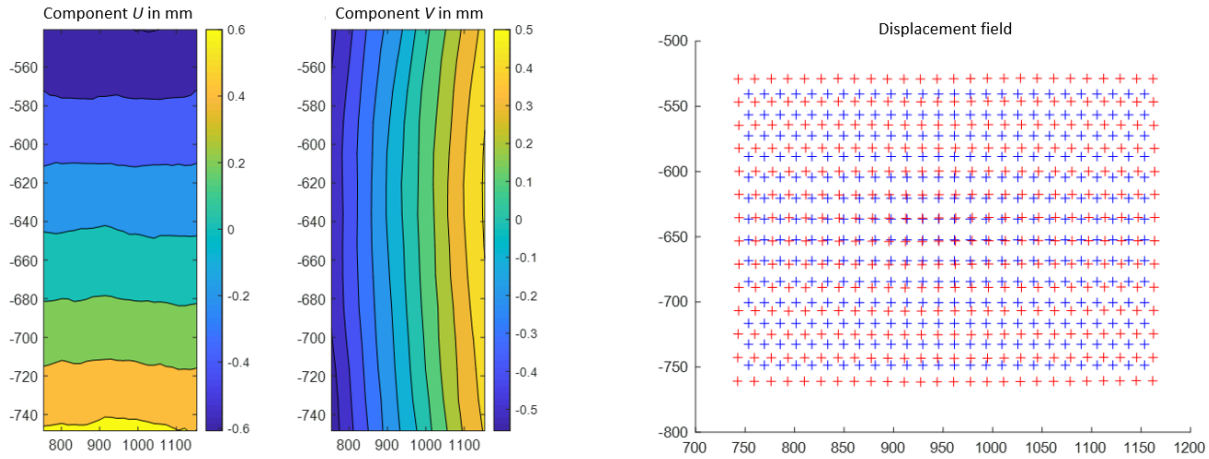

(b)

Figure 2. (a) The region of interest (ROI) measures in the central part of bottle that can be considered almost plane; (b) Visualization of the components U and V of the ROI under 2 bar pressure

The other method, a destructive one, is managed on a biaxial tensile machine also developed at MSME shown on Fig.3 and described in a previous paper of authors [11]. The central zone of the bottle is cut and machined in a water jet machine to produce a cross specimen. To break the symmetry and to generate an heterogenous strain field, a hole is done on the specimen. The location of the hole has been studied in order to optimize the identification process. This process has been detailed in a previous publication of authors [11] and enables to determine all elastic components of the orthotropic material.

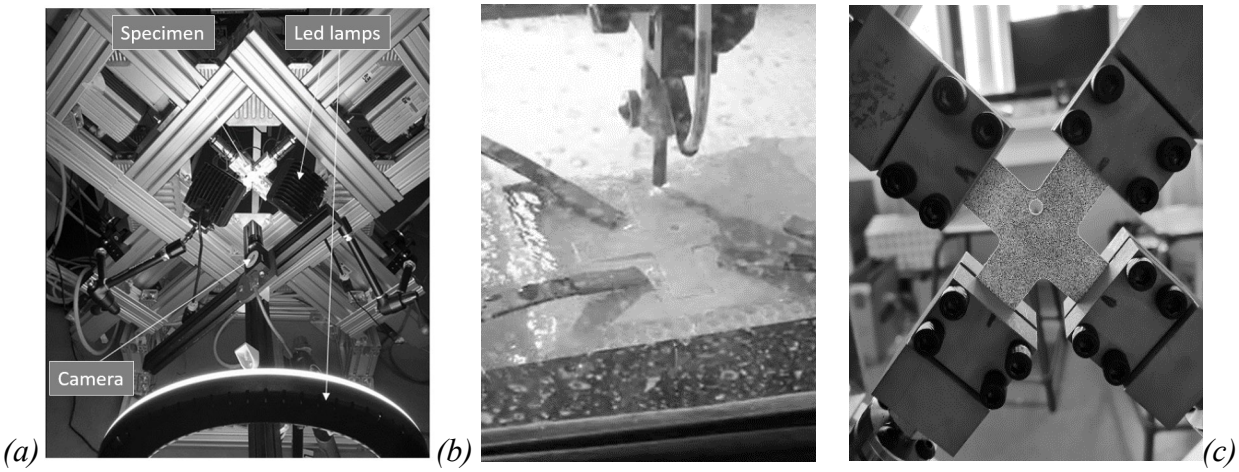

Figure 3. (a) Biaxial testing machine, (b) specimen cut on a water jet machine and (c) biaxial specimen with hole and speckle placed on biaxial machine.

Once again, the DIC method coupled with finite element meshing of the ROI (see Fig.4a) are used but instead of using the virtual field method presented in [11], we carried out a two steps identification. First, we guess some realistic values from literature [9,11] for the material parameters and a finite element calculation is managed imposing as Dirichlet boundary conditions, the DIC displacements on the 4 arms.

After the calculation, the computed global tensile loads F_x and F_y are compared with the measured ones and then 2 correcting factors α_x and α_y are applied to the loads distribution. The second step consists to apply Neumann boundary conditions on the top and left arms with the corrected distribution. We still impose the Dirichlet boundary condition on the bottom and right ones.

From then the set of parameters can be optimized in order to minimize the difference between the DIC displacements measured inside the specimen (Fig.4b) and the finite element displacements depending on the parameter values. This minimization is carried out using the Nelder-Mead simplex algorithm as described in Lagarias et al. [12]. in Matlab. This adaptation of the Finite Element Model Updating (FEMU) method is presented in [13,14] and gives all the material parameters from a single test. In this method, the unknown properties are determined through minimization of Φ with respect to material parameters that is the square difference between the displacement measured (DIC) and the displacement calculated from finite element method (FE) using DIC as boundary conditions.

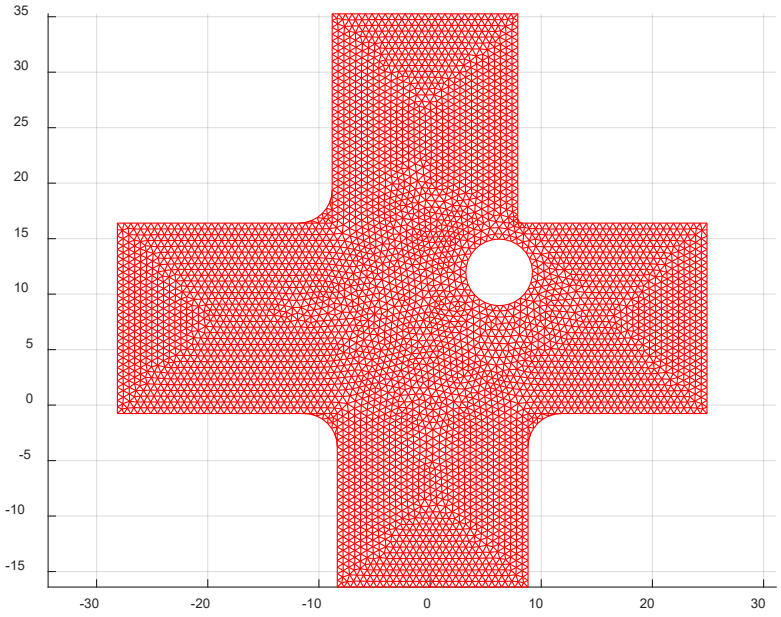

(a)

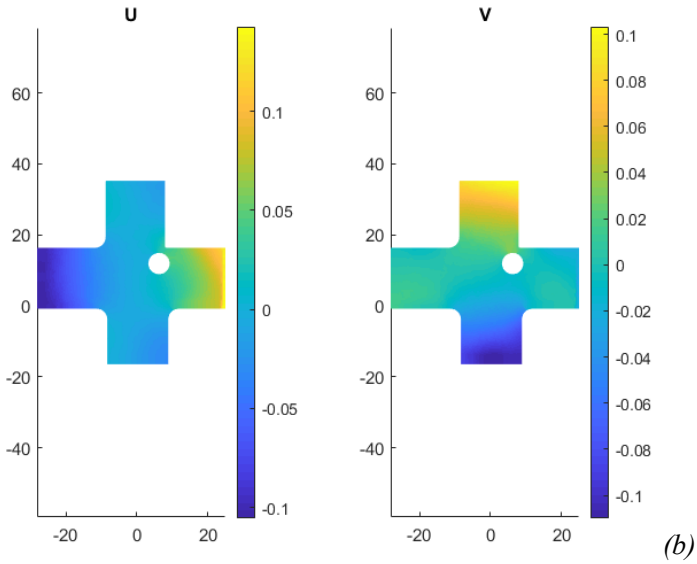

(b)

Figure 4. (a) Mesh of the biaxial specimen with hole and (b) displacement components after an equal-biaxial stretching of the arms.

Results and discussions

First, we will focus on results of the virgin PET N180. Late 90's, Chevalier *et al.* [15] proposed a simple and empiric model to predict the induced modulus from the elongations. The longitudinal modulus E_z was modelled by a 3rd order polynomial function of λ_z while the hoop modulus E_θ was represented by a 2nd order polynomial function of λ_r based on the low number of experimental values higher than λ_r=4. With the value of λ_r equals to 5.15, the predicted hoop modulus would rise to more than 6000MPa which seems to be more than what the measure gives.

Let us first examine the results given by the modified FEMU method from the biaxial tensile test on the cross specimen with a hole. Table 2 summarizes the identified values obtained from the 3 tests managed under identical conditions.

Table 2: *Characteristics of virgin N180 samples*

Characteristics	E_θ **(MPa)**	$\upsilon_{\theta z}$	E_z **(MPa)**	$\upsilon_{z\theta}$	$G_{\theta z}$ **(MPa)**
Mean value	3230	0.43	1790	0.25	1420
Standard deviation	1025	0.05	540	0.16	320
Dispersion	29%	12%	29%	63%	23%

It is interesting to notice that:

- the ratio between the two modulus is conform to what is usually measured [9,11]. Here the ratio is equal to 1.8 between the hoop modulus and the longitudinal one.
- the dispersion is very important for all parameters and this is probably more a consequence of the method (or the measure) rather than a real dispersion from one sample to another. Consequently, we managed the DIC correlation in the arms that supposed to be nearly in simple tension to confirm the modulus and Poisson's ratio.

Figure 5a shows the ROI chosen for this confirmation and Fig.5b confirms that the arm is almost in simple tension because of the regular spacing of the contour lines. One can see that these regular straight lines are only located in the left side of the ROI, so the mean values of the strains must be measured there.

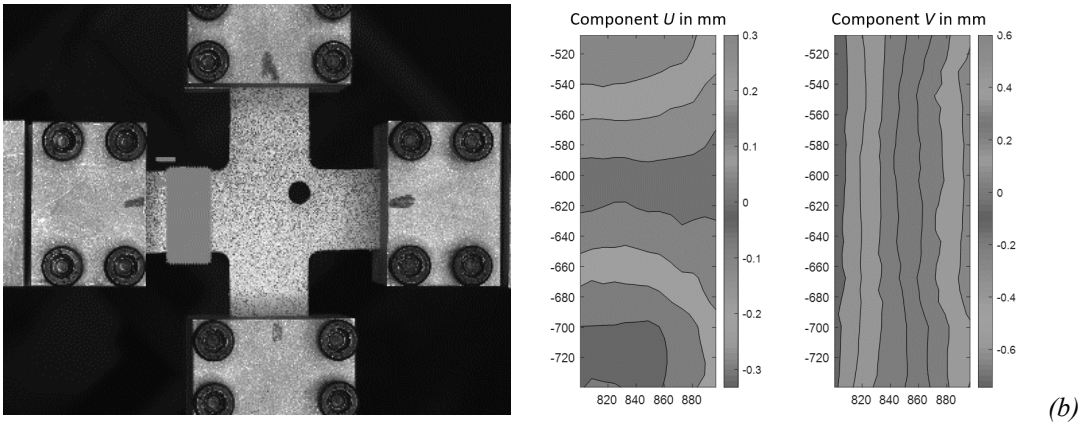

Figure 5. (a) ROI in the arm of the biaxial specimen with hole and (b) displacement component after an equibiaxial stretching of the arms.

Assuming the Poisson's ratio $\upsilon_{\theta z}$ is equal to 0.43, one can manage the series of measure on bottles under pressure. From the displacement fields, we calculate the average deformations in the ROI. 30 rectangle sub-regions are chosen in order to obtain the strains ε_z and ε_θ and their dispersion.

The typical evolution of ε_z and ε_θ as a function of the pressure ($P(i)$ = 0.05 times i in MPa) are illustrated in Fig. 6a. Values are well aligned but fitted lines do not pass exactly through 0 when the pressure is zero. This is often the case because the bottles are never perfectly cylindrical but this geometrical defect disappears after the pressurization. We proceed to a shift (passage of the lines by 0) and proceed to the identification of the elastic modulus at each step as shown on Fig.6b.

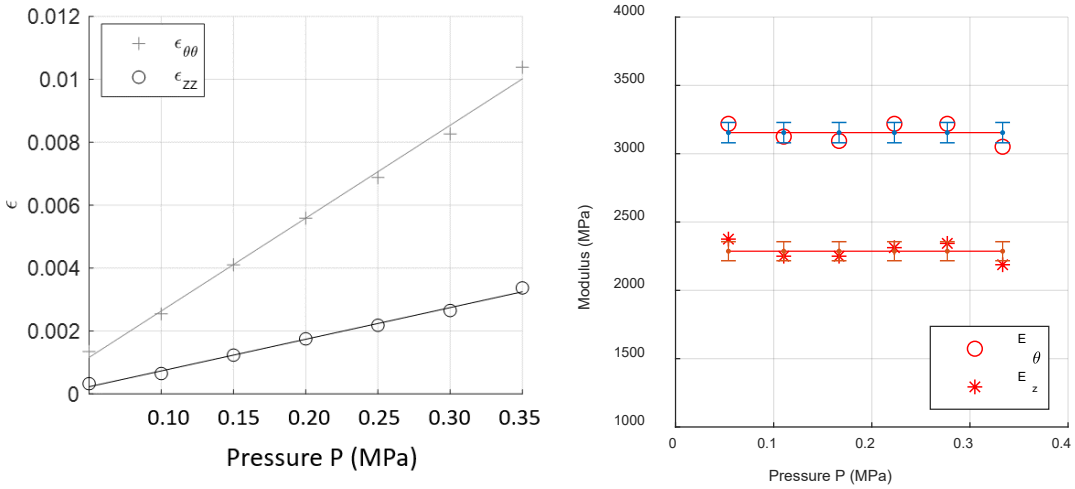

(a) *(b)*

Figure 6. (a) Linear strain evolution versus pressure (b) Induced modulus in virgin N180 PET bottles for $\upsilon_{\theta z}$=0.43

Table 3 shows the values of the longitudinal and circumferential Young moduli in the case of virgin PET N180. Several bottles of the same grade of PET were tested both under pressure and by the arms of the biaxial tensile test. The mean values of E_θ is less than 8% far from the one identified from the global modified FEMU, the E_z modulus is 14% lower. Consequently, the ratio decreases to 1.45, which is smaller than what is usually observed in bottles.

The dispersion of this second series of identification is significantly lower than with the global method: less than 4% for the circumferential module while we reach 12% for the longitudinal module. In literature [15], one observes that there is a less dispersion on the longitudinal modulus than on the circumferential one. Because the preform is stretched longitudinally by a rod, the longitudinal elongation is fixed.

Table 3: Modulus of virgin N180 samples confirmed from the tension in the arms and the bottle under pressure

	E_θ (MPa)	E_z (MPa)
Mean value	2990	2065
Standard deviation	110	240
Dispersion	4%	12%

Considering this identification, we propose to modify the empirical function used in [15] and to choose a 3rd order polynomial function for the modulus E_θ so it varies by passing by a maximum which defines an optimal elongation as one could already see for E_z. The evolution are plotted on Fig.7.

$$E_z = -36.66\lambda_z^3 + 296.9\lambda_z^2 - 396.0\lambda_z + 1313.5$$
$$E_\theta = -83.39\lambda_r^3 + 565.2\lambda_r^2 - 395.14\lambda_r + 1206.5 \quad (3)$$

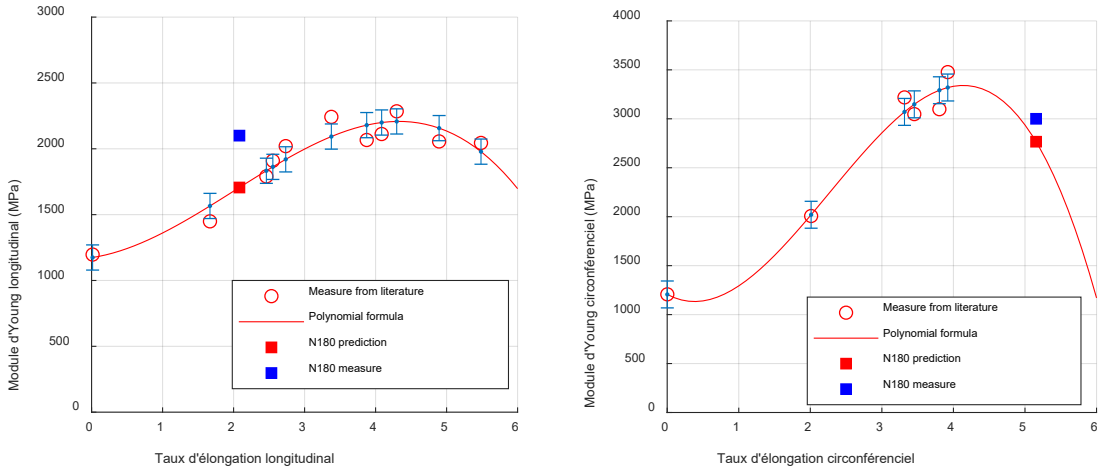

Figure 7. Evolution of modulus E_z and E_θ together with previous experimental data from [15] and values predicted or identified for N180 PET.

Through inflation tests, we carried out a modulus measurement campaign for the three MOPET recycled rates, i.e. 25%, 50% and 100%. Table 4 and Fig.8 show that there is no very clear influence of the recycling rate on the induced modules. It seems that recycled MOPET reinforces the virgin N180 in terms of rigidity: all the modulus of rPET are higher than that of virgin N180.

When we analyze the material sheets (Fig.9 in the appendix), we see that the density and intrinsic viscosity of MOPET are greater than those of N180 (ρ_{MOPET}=0.9kg/dm^3 versus ρ_{N180}=0.83kg/dm^3 and IV_{MOPET}= 0.82-0.87dl/g in front of IV_{N180}= 0.78-0.82dl/g). This is certainly the explanation of why the MOPET bottles are more rigid than the virgin PET N180 one.

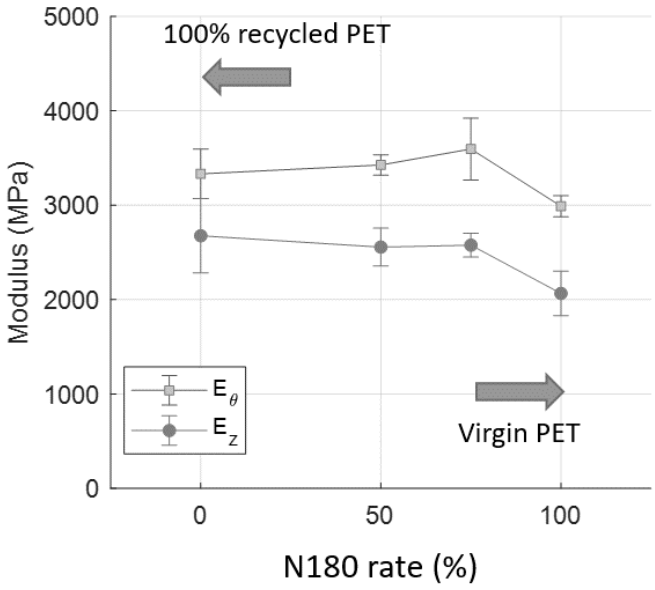

Figure 8: Induced modulus versus virgin N180 PET rate

Table 4: Modulus of rPET samples – influence of the rate of recycled PET

	E_θ (MPa) and dispersion	E_z (MPa) and dispersion
Bottle 1 – 100% N180, 0% MOPET	2990 4%	2065 12%
Bottle 2 – 75% N180, 25% MOPET	3595 9%	2580 5%
Bottle 3 – 50% N180, 50% MOPET	3430 3%	2560 8%
Bottle 4 – 0% N180, 100% MOPET	3330 8%	2680 15%

Conclusion

The measure of the mechanical elastic properties induced by the stretch blow molding process has been carried out on rPET bottles by two different ways: from heterogeneous biaxial tensile tests and from the growth of the bottle under pressure. The second method provides experimental results with less variation and has been used to test the influence of the rate of rPET in the initial preform.

The specific geometry of the blown bottle enriches the data in order to provide a better interpolation of the predicted modulus versus elongation during the process. The influence of the rate of recycled material has been studied. Finally, it appears that in our case, the recycled part reinforce the rigidity in both longitudinal and hoop directions.

Appendix: material characteristics

Property	Unit	Test method	RAMAPET N180 value
Intrinsic Viscosity	dl/g	(K) SDP-15 (R) IND-A-PE-G-IV-01 (Q) CQ–V–1	0.80 ± 0.02
Acetaldehyde	ppm	(K) SDP-21 (R) IND-A-PE-GC-01 (Q) ASTM F 2013	Max 1
Colour L*	-	(K) SDP-05 (R) IND-A-PE-COL-01 (Q) ASTM 6290	Min 78
Colour a*	-	(K) SDP-05 (R) IND-A-PE-COL-01 (Q) ASTM 6290	-3.8 to -0.8
Colour b*	-	(K) SDP-05 (R) IND-A-PE-COL-01 (Q) ASTM 6290	-3.5 to 1
Pellet weight	Pieces/gram	(K) SDP-18 (R) IND-A-PE-PTM-09 (Q) CQ-GA-2	60 ± 5
Fines	Wt%	(K) SDP-60 (R) IND-A-PE-GA-04 (Q) CQ–GA–4	Max 0.05

(a)

Property[a]	Test[b] Method	Typical Value, Units[c]
Pellet Properties		
Crystalline Density Solid Stated pellets	D 1505	1.39 - 1.4 g/cm³
Bulk Density Poured	D 1895	830 ± 30 kg/m³
Bulk Density Vibrated	D 1895	880 ± 30 kg/m³
Melt Density @ 285°C	D 1238 (Note A- Table 2)	1.2 g/cm³
Crystalline Peak Melting Point (T_m) [d]	D 3418	245 ± 5°C
Glass transition point (Tg) (dry)	D 3418	78 ± 2°C
Heat of Fusion [e]	E 793	56 kJ/kg (13 cal/g)
% crystallinity solid Stated pellets		50 ±5 %
Pellet Size		2.5 mm
Pellet Shape		Cylindrical
Moisture content pellets		<0.3%

(b)

Rheology	Value	Unity	Test std.
Viscosity (IV)	0.82 - 0.87	dl/g	ASTM D1238 / ISO 1133)
Other properties	Value	Unity	Test std.
Bulk Density	0.90± 0.50	kg/dm³	Internal
Melt filtration	40	Micron	-
Humidity	< 0.4	%	Internal
Pelletsize (M50)	1 ± 0.2	g	Internal
Black spots (0,5 - 1,0 mm)	< 10	%	Internal / DVS AM356
Black spots (1,0 - 2,0 mm)	< 3	%	Internal / DVS AM356
Black spots (> 2,0 mm)	0	%	Internal / DVS AM356
Acetaldehyde	< 1.0	ppm on chip	ASTM 2013
Dust	< 0.03	%	-
Colour margins Crystallised (specification)	(66) - (74)	L	CieLAB
	(-4.5) - (-1)	a	
	(-7) - (-3)	b	

(c)

Figure 9. (a) and (b) RAMAPET N180 properties (c) MOPET properties

References

[1] F. Welle, Twenty years of PET bottle to bottle recycling—an overview, Resour. Conserv. Recycl. 55 (11) (Sep. 2011) 865–875, https://doi.org/10.1016/j. resconrec.2011.04.009

[2] F. Awaja, D. Pavel. (2005). Injection stretch blow moulding process of reactive extruded recycled PET and virgin PET blends, European Polymer Journal,Volume 41, Issue 11, Pages 2614-2634,ISSN 0014-3057. https://doi.org/10.1016/j.eurpolymj.2005.05.036

[3] N. Torres, J.J. Robin, B. Boutevin. (2000). Study of thermal and mechanical properties of virgin and recycled poly(ethylene terephthalate) before and after injection molding, European Polymer Journal, Volume 36, Issue 10, Pages 2075-2080, ISSN 0014-3057. https://doi.org/10.1016/S0014-3057(99)00301-8

[4] V. Rohart, C. Combeaud. Stretchability above glass transition of mechanically recycled poly(ethylene terephtalate), PET, Polymer, Vol. 257, 2022. https://doi.org/10.1016/j.polymer.2022.125218

[5] A.-D. Le, R. Gilblas, V. Lucin, Y. Le Maoult, F. Schmidt. (2022). Infrared heating modeling of recycled PET preforms in injection stretch blow molding process, International Journal of Thermal Sciences, Vol. 181, 107762, ISSN 1290-0729. https://doi.org/10.1016/j.ijthermalsci.2022.107762

[6] Luo Y.-M., Chevalier L. On induced properties and self heating during free blowing of PET preform. (2019) International Polymer Processing, 34 (3), p. 330 – 338. https://doi.org/10.3139/217.3759

[7] Alvarado Chacon, F., Brouwer, M. T., & Thoden van Velzen, «Effect of recycled content and rPET quality on the properties of PET bottles, part I: Optical and mechanical properties,» Packaging Technology and Science, vol. 33:9, p. 347–357, 2020. https://doi.org/10.1002/pts.2490

[8] Y.M. Luo, T.T. Nguyen, H. Attar, L. Chevalier, F. Lesueur. A new biaxial apparatus for tensile tests on Poly Ethylene Terephthalate optimized specimen at stretch blow molding conditions. Polymer Testing, Elsevier, 2022, pp.107676. https://doi.org/10.1016/j.polymertesting.2022.107676

[9] Anumula, V. S. N., «Prediction of Process-induced Mechanical Properties for Stretch Blow Moulding of PET Bottles,» Queen's University Belfast. Faculty of Engineering and Physical Sciences, 2018.

[10] Leclerc H. , Périé J-N. , Stephane R., François H., «Integrated Digital Image Correlation for the Identification of Mechanical Properties,» Lectures Notes in Computer Sciences, vol. 5496, pp. 161- 171, 2009. https://doi.org/10.1007/978-3-642-01811-4_15

[11] H. Attar, Y.M. Luo, L. Chevalier, T.T. Nguyen, F. Detrez. Identification of anisotropic properties of polymer sheets from heterogeneous biaxial tests. Polymer Testing, Elsevier, 2022, 115, pp.107721. https://doi.org/10.1016/j.polymertesting.2022.107721

[12] Lagarias, J. C., J. A. Reeds, M. H. Wright, and P. E. Wright, Convergence Properties of the Nelder-Mead Simplex Method in Low Dimensions, SIAM Journal of Optimization, Vol. 9, Number 1, pp. 112–147, 1998. https://doi.org/10.1137/S1052623496303470

[13] J. Réthoré, Muhibullah, T. Elguedj, M. Coret, P. Chaudet, et A. Combescure. Robust Identification of Elasto-Plastic Constitutive Law Parameters from Digital Images Using 3D Kinematics. International Journal of Solids and Structures 50, no 1 (2013): 73-85. https://doi.org/10.1016/j.ijsolstr.2012.09.002

[14] T. Marwala, I. Boulkaibet, S. Adhikari. Probabilistic Finite Element Model Updating using Bayesian Statistics. Application to aeronautical and mechanical engineering. 1st edition, John Wiley & Sons Ltd, Chichester, 2017. https://doi.org/10.1002/9781119153023

[15] L. Chevalier, Y. Marco, G. Regnier. Modification des propriétés durant le soufflage des bouteilles plastiques en PET, Mécanique & Industries, vol. 2(3), pp. 229-248, 2001. https://doi.org/10.1016/S1296-2139(01)01094-6